Preparation of 4-Arylpyridine-2,6-Dicarboxylic Acids *via* Microwave-assisted Suzuki Coupling

A Thesis Presented to

the Faculty of the Department of Chemistry

University of Houston

In Partial Fulfillment

of Requirements for the Degree

Master of Science Degree

By

Thao Shirley Nguyen

May 2013

Preparation of 4-Arylpyridine-2,6-Dicarboxylic Acids *via* Microwave-Assisted Suzuki Coupling

_____

Thao Shirley Nguyen

APPROVED:

_____

Dr. Scott Gilbertson
Advisor

_____

Dr. Jeremy May
Committee Chairperson

_____

Dr. Olaf Daugulis

_____

Dr. Robert Fox

_____

Dr. Arnold Guloy

_____

Dr. Dan Wells
Dean, College of Natural Sciences and Mathematics

Acknowledgements

I would like to express my most sincere appreciation to my advisor Dr. Scott Gilbertson for his help and guidance during my three years. “Thank you, boss. I could not have made it this far without you.”

I also would like to express my gratitude to Dr. Anton Agarkov for all his help in the lab and for all the chemistry discussions (especially the most intense ones).

A big hug to my lab members.

Preparation of 4-Arylpyridine-2,6-Dicarboxylic Acids *via* Microwave-assisted Suzuki Coupling

An Abstract of a Thesis Presented to

the Faculty of the Department of Chemistry

University of Houston

In Partial Fulfillment

of the Requirements for the Degree

Master of Science Degree

By

Thao Shirley Nguyen

May 2013

Abstract

Protein crystallography is a useful tool to elucidate protein structures to the atomic level. X-ray crystallography requires high-quality diffracting crystals, which can be difficult to obtain, especially for proteins. Proteins are fragile, sensitive to external changes, highly heterogenous and large. In addition, protein-protein interactions are weak and scattered over a large surface area. To bring the large, heterogenous protein molecules into an ordered arrangement is a challenge. Several approaches have been explored to better promote protein crystal formation; for instance small molecules, polymers, and metal ions. Recently, organo-lanthanide complexes have been reported to work well. Lanthanide complexes have two advantages over the other approaches: 1) if a lanthanide complex is successfully incorporated into a protein, the derivatized protein will luminesce under UV light, and 2) lanthanide complexes possess large anomalous factors which are useful in X-ray crystallography. Only two classes of organo-lanthanide complexes have been reported for use in protein crystallography; one is based on cyclen and the other is based on dipicolinic acid. Herein, we wish to present our preparation of eight derivatives of dipicolinic acid using microwave-assisted Suzuki coupling. We found that the Suzuki reaction worked best at 140 ^{o}C for 40 minutes and the best conditions for the hydrolysis of the diesters were 14 equivalents of LiOH in 3:1 MeOH/H_2O. Six of the compounds exhibited limited solubility, whereas 4-(4-carboxyphenyl)pyridine-2,6-dicarboxylic acid and 4-(4-aminophenyl)pyridine-2,6-dicarboxylic acid showed improved solubility. Sterically hindered boronic acids reacted less efficiently and highly

electron-poor boronic acids did not react at all. The eight compounds will be used in the preparation of lanthanide complexes, which will be screened against nine proteins.

Table of Contents

Abbreviations

dGMP	deoxyguanosine monophosphate
DMAP	4-dimethylaminopyridine
DO3A	10-(2-hydroxypropyl)-1,4,7,10-tetraazacyclododecane-1,4,7-triacetic acid
dpa	dipicolinate
dppf	1,1'-bis(diphenylphosphino)ferrocene
DOTA	1,4,7,10-tetraazacyclododecane-1,4,7,10-tetraacetic acid
DOTMA	*a,a',a", a'''*-tetramethyl-1,4,7,10-tetraazacyclododecane-1,4,7,10-tetraacetic acid
EDC	1-ethyl-3-(3-dimethylaminopropyl)carbodiimide
$EtGua^+$	ethylguanidinium cation
EtOAc	ethyl acetate
HEWL	hen egg-white lysozyme
HM-PGA	high molecular weight polyglutamic acid
HPDO3A	10-(2-hydroxypropyl)-1,4,7,10-tetraazacyclododecane-1,4,7,10-tetraacetic acid
HPLC	high-performance liquid chromatography
LC/MS	Liquid chromatography/Mass spectrometry
LM-PGA	low molecular weight polyglutamic acid
MeOH	methanol
μw	microwave

NMR	nuclear magnetic resonance
PEG	polyethylene glycol
UV	ultraviolet

1. Introduction

The common bottleneck in protein crystallography is to obtain high-quality diffracting crystals. More often in protein crystallization attempts, protein molecules precipitate as amorphous solids or stay in solution. The number of variables that influences protein crystal formation is large and unfortunately, there is no universal protocol for crystallizing proteins but it is rather a trial-and-error process. Physical, biochemical, and chemical factors that affect protein crystallization include protein purity and homogeneity, precipitant, pH, additive, and temperature, to name a few. Furthermore, proteins can be fragile and sensitive to their environment; consequently, the challenge lies in finding optimal crystallization conditions which also leave the protein intact.

Two widely used techniques to crystallize proteins are vapor diffusion (sitting-drop and hanging-drop) and batch crystallization.[2,3] The theory behind these methods is to slowly bring protein concentration to supersaturation and with luck, the protein nucleates spontaneously from the solution and continues to grow. Since the line between the supersaturated state and the precipitation zone is fine, the protein may precipitate instead of crystallize.

In a typical vapor diffusion experiment, a container is partially filled with precipitant solution at a certain concentration and pH.[3] A drop consisting of a microliter-volume of the protein solution at a certain concentration (usually 5-50 mg/mL) and an equal volume of the precipitant solution is placed, separate from the precipitant reservoir, in the container. The container is then sealed to allow equilibrium to be reached between the precipitant reservoir and the drop. Initially, the drop is undersaturated. As the system approaches equilibrium, the concentrations of protein and precipitant in the drop increase until supersaturation is reached

which in theory allows spontaneous nucleation. The role of the precipitant is to promote crystallization; however, in many cases, it fails to do so. In fact, in a 2002 report, the percentage of successful crystallization was estimated to 26%.[4] Therefore, alternative approaches in promoting crystallization are necessary. One solution is the addition of an additive which will act as the principle precipitant. Small molecules[5,6] , polymers[7,8] as well as mono- and divalent metal ions[9,10] have been demonstrated to work well. Herein is a selection of recent studies of the above mentioned additives described.

McPherson *et al.* carried out laborious work in search for classes of small molecules that promote crystallization. All together, 500 small molecules and 81 proteins were screened in roughly 50000 crystallization trials.[5,11] The small molecules were added as mixtures based on their similarity in structure and chemistry. They included bioactive and chemical compounds, which could affect the physical properties of the proteins, such as solubility, surface and inter-macromolecular interactions. An interesting feature of the studies is that only two crystallization conditions were used, one was based on 30% PEG 3350 and the other on 50% Tacsimate™ (mixture of seven organic acids) at pH 7. Small molecules with charged functional groups such as dicarboxylic acids and diamines or both were found to better promote crystallization. Crystal structures of selected derivatized proteins displayed electrostatic interactions between the proteins and the additives. Further, the latter served as bridges to connect protein molecules together. In some cases, however, the small molecules were not found in the crystallized proteins but rather the precipitant (example thaumatin with protamine as additive), or they somehow induced conformational changes in the proteins, which were more favorable towards crystal formation (hen egg-white lysozyme with different additives).[11] In other cases, they bound tightly to the active sites of the proteins

(bovine ribonuclease A with dGMP as additive).[11] Some proteins were found to co-crystallize with one of the components in the small molecules mixture suggesting that they could select from a mixture of structurally and chemically similar compounds the most suitable for self-assembly (bovine trypsin with mellitic acid).[11]

McPherson *et al.* also investigated the capability of polymers in promoting protein crystallization. Based on the successful reports of PEG 400 as precipitant, they turned to water-soluble polymers of different (rather high) molecular weights, such as polyacrylic acid 5100 and 2100, polyvinyl alcohol 15000 and polyethylene glycol 2000, at varied concentrations and pHs.[7] Of the 24 proteins tested, 14 yielded crystals. Although most of the crystallized proteins were not of high quality, the studies demonstrated that polymers could be used as additives to promote crystallization. Brzozowski *et al.* screened polyglutamate-gluosamine of low and high molecular weight against 13 proteins, ten of which had not previously been crystallized.[8] Amide coupling of low and high molecular weight polyglutamic acid (LM-PGA and HM-PGA, respectively) with glucosamine using EDC/DMAP afforded glucosamine-LM-PGA and glucosamine-HM-PGA, respectively. The results showed that in 2:1 mol ratio of glucosamine:PGA, the solubility of the polymer was improved. Low and high molecular weight glucosamine-PGAs promoted crystallization to similar extent. Further, the results also showed that the PGA derivatives worked well as stand-alone additives, in combination with PEG or in conjunction with other additives. At the moment of writing, the crystal structures had not been published.

Use of sole metal ions to encourage protein crystallization is a difficult approach since protein surfaces are highly heterogenous and protein-protein interactions are scattered over a large area; to precisely incorporate metal ions for proper coordination by proteins is a

challenge. Therefore, surface-mutated proteins are often used in metal-mediated protein crystallization. Crystallization of cytochrome cb_{562} studied by Tezcan *et al.* utilized a mutated form of the protein, called His^4-cb_{562}, which was modified at four positions 59, 63, 73 and 77 with histidines.[9,10] Using Zn^{2+}, Ni^{2+} and Cu^{2+}, they demonstrated how the assembly of His^4-cb_{562} monomers could be controlled by different metal ions. At intermediate concentrations of Zn^{2+} and His^4-cb_{562}, dimeric structure (Zn_2(His^4-cb_{562})$_2$) was observed whereas at high concentrations, the momomers rearranged into tetrameric structure (Zn_4(His^4-cb_{562})$_4$) and thereby fully occupy the metal ion. The results showed that the self-assembly of the proteins is controlled by thermodynamics rather than kinetics. With Ni^{2+} and Cu^{2+}, the monomers formed a different dimeric structure with Cu^{2+} (Cu_2(His^4-cb_{562})$_2$) and trimeric structure with Ni^{2+} (Ni_2(His^4-cb_{562})$_3$).

Recently, organo-lanthanide complexes have emerged successfully in promoting protein crystallization.[11,12,13,14,15] In a way, lanthanide complexes interact with proteins in a similar manner as small molecules (*via* intermolecular electrostatic interactions albeit through the organo moiety). However, lanthanide complexes have two advantages over small molecules, polymers and divalent metals. One is that the derivatized protein crystals can be visualized with UV light thanks to the physico-chemical properties of the lanthanides. In addition, lanthanides also assist in solving X-ray structures due to their large anomalous factors.

The organo component in an organo-lanthanide complex sensitizes the lanthanide ion as such the latter displays enhanced luminescence under UV light. The organo compound also provide anchor sites to which other molecules can bind. In a 2008 report, Pompidor *et al.* provided a description of the interaction of tris(dipicolinate)-lanthanide salt **1** (Figure 1),

hereafter called $[Ln(dpa)_3]^{3-}$, and hen egg-white lysozyme (HEWL).[12] The complex bound to HEWL intermolecularly *via* hydrogen bonding between carboxyl groups of the complex and arginine residues of the protein. Co-crystal of the protein-complex luminesced under UV light (λ_{ex} = 254 nm) due to the indirect excitation of Eu^{3+} or Tb^{3+} by dpa.

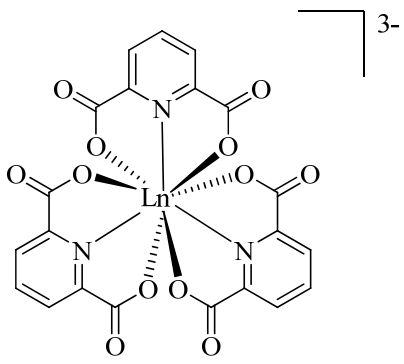

1

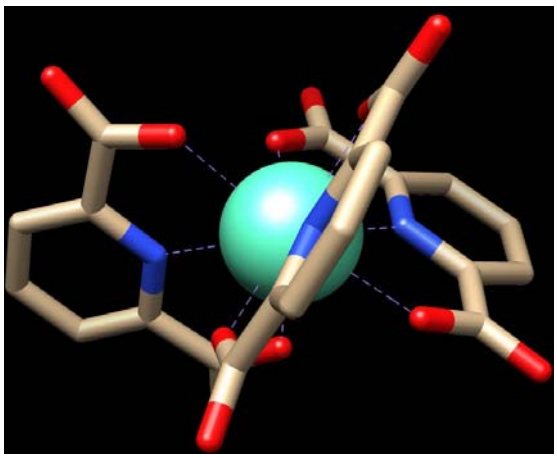

Figure 1. Representative structure of tris(dipicolinate)-lanthanide complexes which have been used in protein crystallography. Left: General structure of $[Ln(dpa)_3]^{3-}$. Right: 3-D representation of $[Eu(dpa)_3]^{3-}$. Three dipicolinates coordinate to Eu^{3+} in a propeller-like fashion. Red = oxygen, blue = nitrogen, grey = carbon, cyan = Eu^{3+}. Hydrogens have been omitted for clarity. Reproduced from ref 12 using CHIMERA.

To further understand how $[Ln(dpa)_3]^{3-}$ (**1**) bound to HEWL and how strong the complexation was, $EtGua^+$ ion mimicking guanidinium side chain of arginine was co-crystallized with the complex. The co-crystal structure of $(EtGua)_3[Tb(dpa)_3]\cdot 2H_2O$ revealed the participation of the primary amine and imine of guanidinium acting as hydrogen-bond donors and of two carboxylates from the same or different dipicolinate acting as hydrogen-bond acceptors. The strong affinity of $EtGua^+$ for $[Tb(dpa)_3]^{3-}$ also existed in solution. To determine the association constants of complexation, eight ^{1}H-NMR titration experiments were conducted, each experiment varied in either the initial concentration of Tb^{3+} or in the counterion of $[Tb(dpa)_3]^{3-}$. As the concentration of EtGuaCl increased, the ethyl protons steadily shifted upfield until the solution was saturated with EtGuaCl (approximately 24

equivalents). By fitting the experimental data to the corresponding calculated shifts using least-square method, four association constants could be determined. The average overall association constant for the complexation is $K = K_1K_2K_3 \approx 61\ (\pm 11) \times 17\ (\pm 4) \times 4\ (\pm 0.5) \approx 10^{3.7\ (\pm 0.2)}$, where K_1, K_2 and K_3 are association constants of $(EtGua)[Tb(dpa)_3]^{2-}$, $(EtGua)_2[Tb(dpa)_3]^{-}$, $(EtGua)_3[Tb(dpa)_3]$, respectively.

Following their successful results, Pompidor *et al.* attempted to co-crystallize **1** with other proteins, namely thaumatin, turkey egg-white lysozyme, urate oxidase, xylanase and porcine pancreatic elastase.[13] In all cases, the proteins bound to the complex through hydrogen-bonding between hydrogen-bond donors of the protein and the carboxylate oxygens of the dipicolinate. Moreover, co-crystal structures of derivatized HEWL and xylanase, respectively, revealed a new crystal form for the proteins whereas the rest of the derivatized proteins crystallized in their native form.

Talon *et al.* expanded the idea of using $[Ln(dpa)_3]^{3-}$ to crystallize proteins to be generally applicable to derivatives of dipicolinic acid.[14] Three (4-substituted)-4-triazolopicolinic acids were prepared *via* copper-catalyzed azide-alkyne cycloaddition (Figure 2). HEWL readily co-crystallized with charged (**2**, **3**) and neutral (**4**) lanthanide complexes in its native crystal form. The co-crystal structure revealed, in addition to the electrostatic interactions, additional π-π interactions between the triazole ring of the complex and phenyl ring of tryptophan. Consequently, derivatized HEWL could be obtained at lower concentrations of lanthanide complexes. Crystallization of derivatized thaumatin was successful with charged (**2**, **3**) lanthanide complexes (also at lower concentrations of the complexes, although it is unclear why it was the case) but it failed to co-crystallize with the neutral (**4**) lanthanide complex. This is thought to be because, unlike HEWL, thaumatin does

not have accessible hydrophobic residues to establish interactions with the uncharged complex.

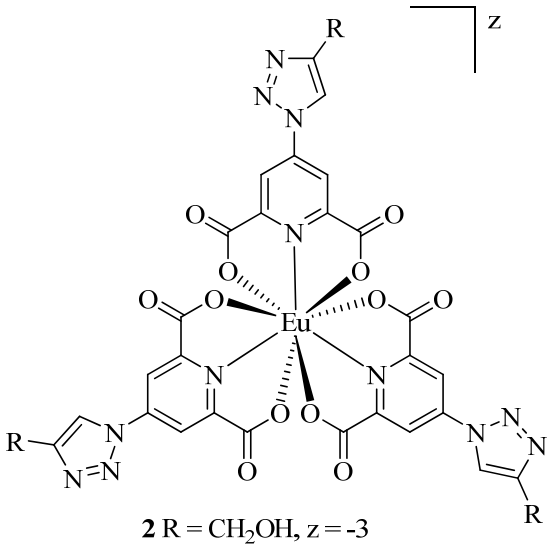

2 R = CH_2OH, z = -3
3 R = CH_2CH_2OH, z = -3
4 R = $CH_2N^+(Me)_2CH_2CH_2OH$, z = 0

Figure 2. Structural variation of [tris(dipicolinate)-Eu]$^{3-}$.

Other chelating agents for Ln^{3+} that have been successfully employed in protein crystallography are based on cyclen (tetraazacyclododecane) (Figure 3, left).[15] Unlike dipicolinic acid, wherein three tridentate dipicolinates coordinate to one Ln^{3+}, cyclen acetic acid derivatives are septadentate (**6**) or octadentate (**5**, **7**, **8**) forming a cage around one Ln^{3+}. This leaves lanthanide ion with unoccupied sites, which can be filled by water molecules (Figure 3, right).

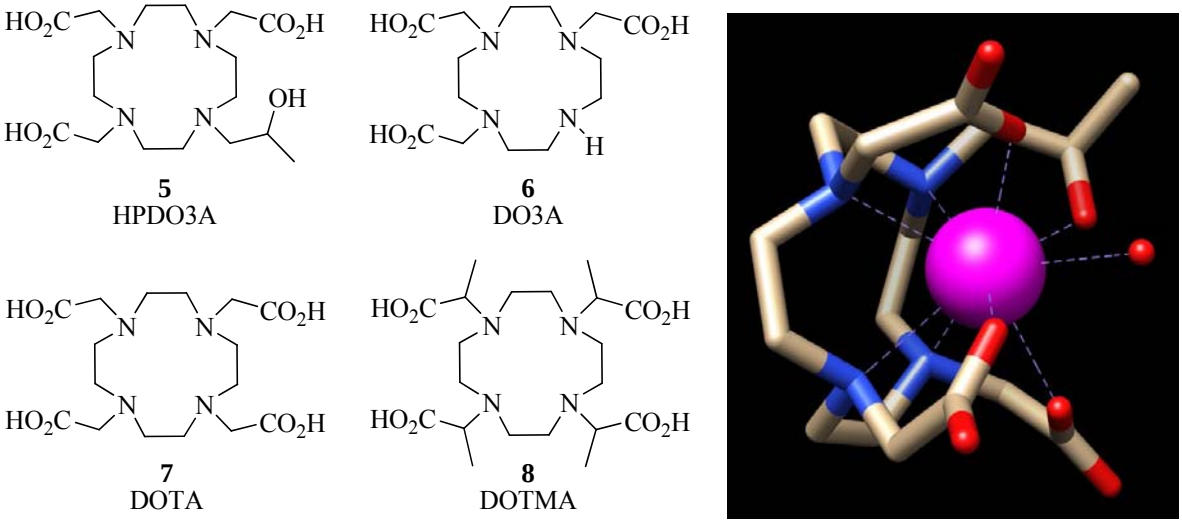

Figure 3. Examples of cyclen derivatives used as chelating agents for Ln^{3+}. Left: Except for DO3A, which is a septadentate ligand, HPDO3A, DOTA and DOTMA are octadentate. Right: 3-D representation of Gd-HPDO3A complex. Water forms a ninth ligand to the lanthanide ion. Red = oxygen, blue = nitrogen, grey = carbon, magenta = Gd^{3+}. Hydrogens have been omitted for clarity. Reproduced from ref 6 using CHIMERA.

Gd-**5** complex is neutral and co-crystallizes with HEWL at high concentrations without damaging the derivatized crystal. Two Gd-**5** complexes occupy two sites of one HEWL molecule. At each binding site, the hydrophobic cyclen interacts with tryptophan of the protein while the hydrophilic carboxylates and hydroxyl group form a hydrogen-bonding network with hydrophilic residues of the protein.[15a] At low concentrations of the Gd-**5** complex, only one site is occupied. Gd-**5** complex also readily co-crystallizes with catalase and urate oxidase. Replacing Gd^{3+} for Lu^{3+} or Yb^{3+} did not affect the binding mode of the complex with the protein.[15c] Similarly, derivatized HEWL, urate oxidase and chimeric ornithine carbamoyl transferase could be obtained with complexes of Gd^{3+} and other cyclen derivatives.[15b,15d]

Sensitized lanthanide complexes used in protein crystallography is still an unexplored field, which we would like to investigate. Employing dipicolinic acid derivatives is a

promising path towards achieving protein crystal structures. Dipicolinic acid and its derivatives have several advantages over cyclen derivatives. They strongly and fully coordinate to the lanthanide ion allowing the possibility to crystallize proteins at low concentrations and disallowing water to coordinate to the ion. They are noninvasive to HEWL (as opposed to HPDO3A) and are able to form new crystal forms with proteins. Our interest and quest were therefore to explore other derivatives of dipicolinic acid to be crystallized with lanthanides. We were particularly interested in pursuing symmetrical adducts of dipicolinic acid as symmetry will reduce the number of different atoms diffracted in X-ray crystallographic experiments. Consequently, a series of 4-aryl dipicolinic acids were constructed from 4-bromo dipicolinic acid and different aryl boronic acids *via* Suzuki cross-coupling. Among metal-catalyzed cross-coupling reactions for C-C bond formation, Suzuki-Miyaura coupling is probably one of the most widely used. It relies on palladium(0) to mediate the construction of biaryls from aryl halides and organoboron compounds.[16] The proposed mechanism for the Suzuki coupling is given in Scheme 1.

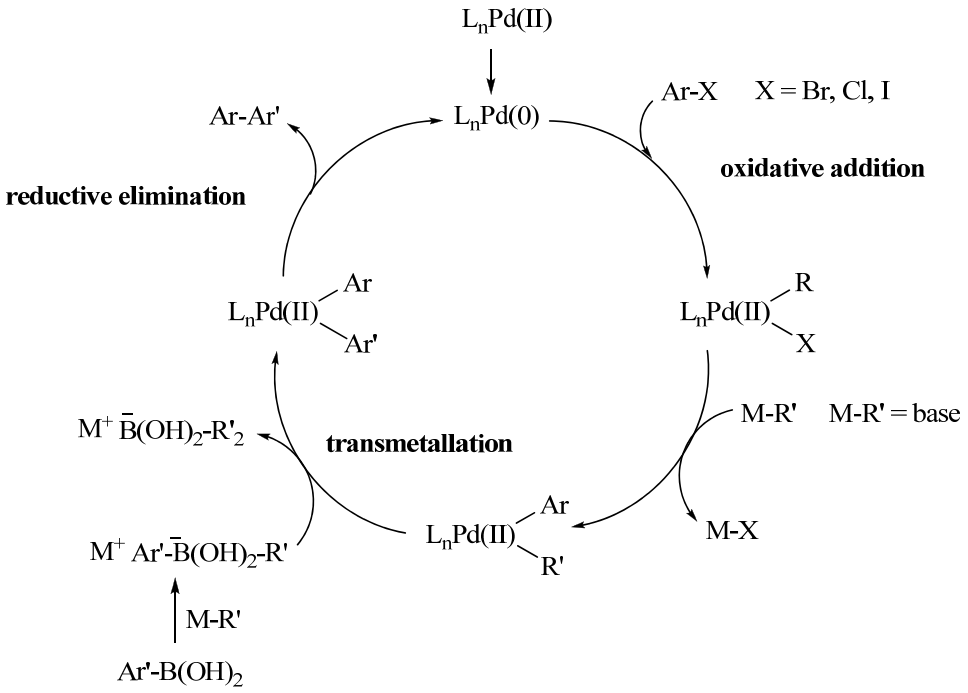

Scheme 1. Proposed mechanism of Pd(0)-catalyzed Suzuki coupling reactions.

There are a tremendous number of papers reporting the Suzuki coupling under different reaction conditions, all of which are to improve the reaction and/or to address incompatibility of unreactive boronic acids and/or aryl halides. Conventional Suzuki coupling is carried out under inert atmosphere. However, the reaction has demonstrated to work well in microwave without providing inertness.[17] Microwave-assisted Suzuki coupling is convenient; therefore, we chose this protocol in our preparation of dipicolinic acid derivatives.

2. Results and Discussion

Our scaffold dimethyl 4-bromopyridine-2,4-dicarboxylate (**10**) was obtained in one step by brominating chelidamic acid **9** with PBr_5 followed by esterification with methanol (Scheme 2).[18]

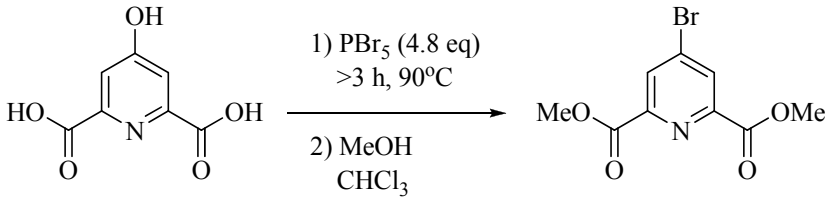

9 **10**

Scheme 2. Synthesis of the starting material 4-bromopyridine-2,6-dicarboxylate (**10**).

Aryl-aryl coupling of **10** with boronic acids *via* microwave-assisted Suzuki coupling afforded the corresponding 4-arylpyridine-2,6-dicarboxylates. Hydrolysis of the diesters yielded diacids in low to moderate overall yields (Table 1, entry 1–8).

In an attempt to optimize the Suzuki coupling, several parameters were investigated. Our initial approach at 120°C showed conversion of **10** to coupling products as indicated by HPLC and LC/MS. With 10 degree increment, the reaction showed higher conversion and was further improved at 140°C. Longer reaction times also seemed to enhance the product formation (Table 1, entry 4 and 6). However, as we increased the reaction times beyond 60 minutes, the catalyst began to decompose. Additional optimization by increasing the amount of boronic acid from 1 equivalent to 1.5 equivalents did not affect the coupling. Unfortunately, we could not optimize the base, the solvent or the catalyst due to time constraints.

In addition to the above mentioned boronic acids (Table 1, entry 1–8), we also tried to couple several fluorine-containing phenylboronic acids with **10** (Table 1, entry 9–11).

Difluorophenyl adducts were detected by HPLC and LC/MS whereas tetrafluorophenyl boronic acid failed to undergo Suzuki coupling even at elevated temperatures and prolonged reaction times. The results could be explained by electronic effect wherein highly electron-deficient substrates are inactive towards Pd-mediated coupling. As reasoned by Sakai *et al.* in the case of pentafluorophenyl boronic acid,[19] we believed that the reason for the inactivity of tetrafluorophenyl boronic acid could be in the transmetalation or in the reductive elimination step. The exact cause is beyond the scope of this thesis and was therefore not investigated. Steric effects in Suzuki coupling were also observed. Higher yield was obtained for the less sterically hindered boronic acid (Table 1, entry 3 and 4).

The conditions of the hydrolysis of the diesters were optimized to be 14 equivalents of LiOH in 3:1 MeOH/H_2O. At lower equivalents, partial hydrolysis to monoacids was observed on HPLC. Same results were obtained with 6.5 equivalents of K_2CO_3 in 2:1 MeOH/H_2O.

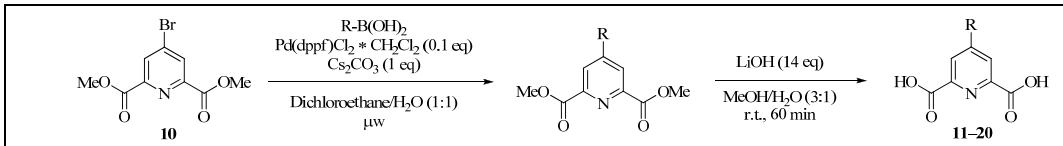

Entry	R-B(OH)$_2$	Temperature (^{o}C)	Time (min)	Product	Overall yield (%)
1	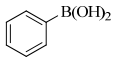	140	20	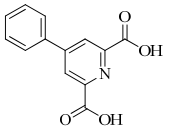 **11**	43
2	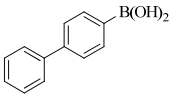	140	30	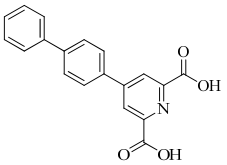 **12**	35
3	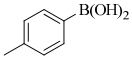	140	40	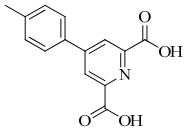 **13**	71
4	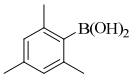	140 140	7 40	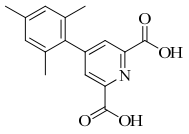 **14**	19 61
5	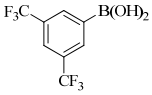	120	10	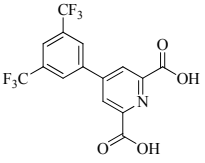 **15**	1
6	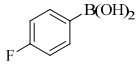	120 140	10 40	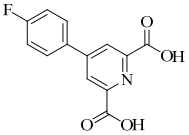 **16**	1 27

Table 1. Reaction conditions and overall yields. The reaction progress was followed on HPLC.

Table 1 continued.

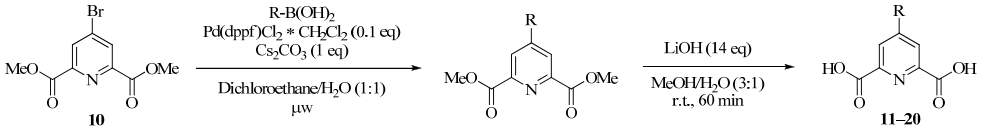

7	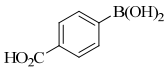	140	40	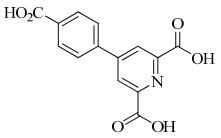 **17**	28
8	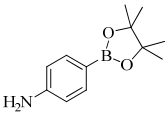	140	40	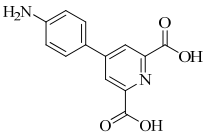 **18**	pending
9	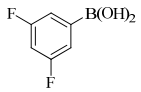	120	14	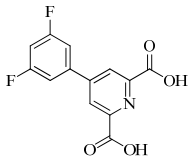 **19**	not isolated
10	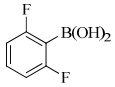	140	40	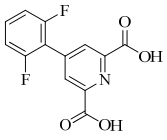 **20**	not isolated
11	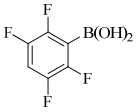	140	>60	-	-

In conclusion, eight 4-arylpyridine-2,6-dicarboxylic acids were synthesized *via* microwave-assisted Suzuki coupling. To the best of our knowledge, only two compounds have been previously made (**11** and **17**). Compounds **11**–**16** displayed very limited solubility in water. To address this issue of insolubility, compounds **17** and **18** containing a carboxyl and an amino group, respectively, were synthesized. Both compounds exhibited improved solubility which is important in the preparation of lanthanide complexes and in the protein

crystallization. If the complexes are successfully prepared, they will be used in protein crystallization. At the time of writing, the results were still pending.

3. Future directions

4-arylpyridine-2,6-dicarboxylic acids can be further explored. However, hydrophilicity should be taken into consideration as such polar groups should be incorporated (Figure 4).

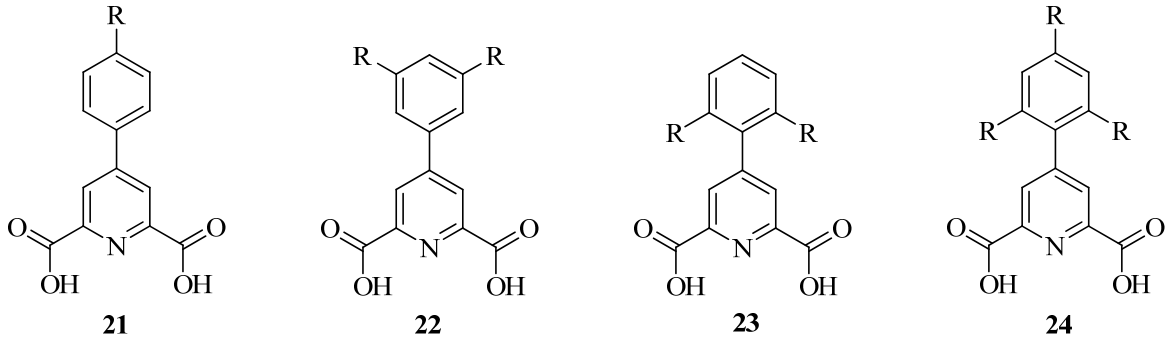

Figure 4. Possible substituted 4-arylpicolinic acids to be explored. R = polar groups, such as CO_2H, NH_2, OH, $CONH_2$, guanidinium, SO_3H.

In addition, we can employ the chemistry of heterocycles in click chemistry by coupling 4-azidopyridine-2,6-dicarboxylic acid with different terminal and internal alkynes (Scheme 3).

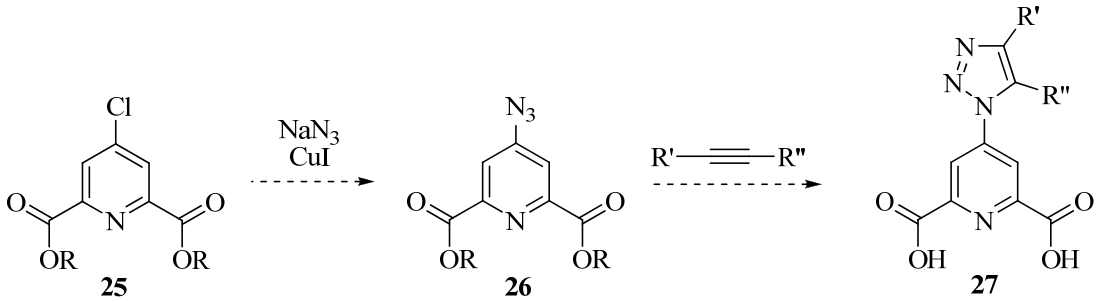

Scheme 3. Use of click chemistry to form triazoles.

We can also prepare secondary amines which will provide more flexibility to bind proteins (Scheme 4).

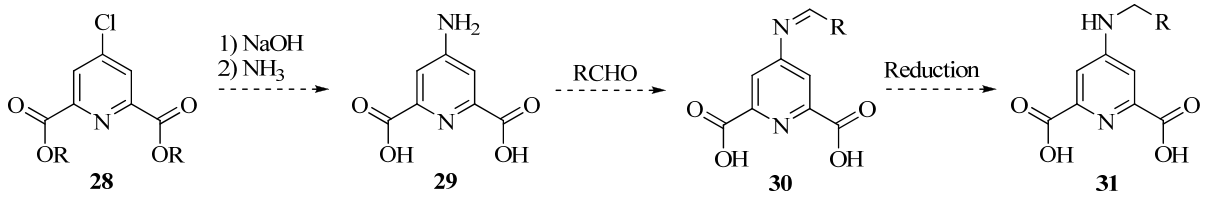

Scheme 4. Secondary amines *via* Schiff base.

4. Experimental procedure

4.1 General

All chemicals were used without further purification. Analytical HPLC was carried out on Thermo Betabasic-8 (5 μm, 4.6×100 mm) column with flow rate 0.8 mL/min. Preparative HPLC was performed on XBridge^{TM} C_{18} (5 μm, 19×150 mm) column with flow rate 10 mL/min. Same solvent system was used for analytical and preparative HPLC, which is 0.1% TFA in H_2O and 0.1% TFA in MeCN. Low-resolution mass spectra were obtained on Thermo Finnigan Surveyor System equipped with PDA Plus Detector and Single Quadrupole LC/MS using Betabasic-18 (5 μm, 2.1×50 mm) column. NMR spectra were obtained on JEOL ECX-400P and processed using software Delta 4.3.6.

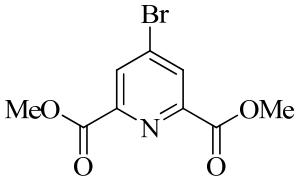

10

Dimethyl 4-bromopyridine-2,6-dicarboxylate (10).[18] Chelidamic acid (6.08 g, 30 mmol) and PBr_5 (62 g, 144 mmol, 4.8 eq) were heated at 90^{o}C for 3 h during which PBr_5 melted and chelidamic acid formed a glue-like melt. Chloroform (50 mL) was added to the reaction mixture upon which a solid precipated. The mixture was filtered, and the filtrate was cooled to 0^{o}C. At this temperature, MeOH was added dropwise. The white solid was collected and recrystallized from MeOH to give the titled compound as white crystals (5.2 g, 19 mmol, 63%). ^{1}H-NMR (400 MHz, $CDCl_3$): δ (ppm) 8.44 (s, 2H), 4.01 (s, 6H); ^{13}C-NMR (100 MHz, $CDCl_3$): δ (ppm) 164.1, 149.1, 135.3, 131.4, 53.6; LRMS (ESI) calcd for

$C_9H_8BrNO_4$: m/z 274.0 (M + H), found: 273.7 (100), 275.7 (99), retention time = 10.06-10.60 min.

General procedure for the syntheses of 4-arylpyridine-2,6-dicarboxylic acids (11–18).[17] Dimethyl 4-bromopyridine-2,6-dicarboxylate **10**, boronic acid (1 eq or 1.5 eq), Pd(dppf)Cl_2·CH_2Cl_2 (10 mol%) and dichloroethane were added to a microvial. Aqueous Cs_2CO_3 (1 eq) was added to the mixture. The reaction was run in microwave reactor. After cooling to room temperature, the reaction mixture was extracted with EtOAc. The combined organic layer was washed with water, dried over $MgSO_4$, filtered and concentrated *in vacuo*. The crude material was flashed through silica gel in hexane/EtOAc.[20] The product was dissolved in 0.7 M LiOH·H_2O in MeOH/H_2O 3:1 (14 eq). The reaction was run at room temperature for 1 h. The reaction mixture was cooled to 0°C, then acidified with aqueous HCl during which a precipitate was formed. Water was removed and the residue was purified by reverse HPLC.

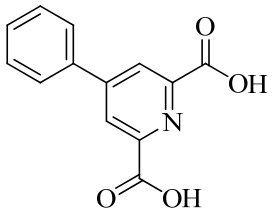

11

4-Phenylpyridine-2,6-dicarboxylic acid (11). Dimethyl 4-bromopyridine-2,6-dicarboxylate **10** (260 mg, 0.95 mmol), phenylboronic acid (116 mg, 0.95 mmol), Pd(dppf)Cl_2·CH_2Cl_2 (78 mg, 0.095 mmol, 10 mol%), dichloroethane (2 mL), aqueous Cs_2CO_3 (2 mL, 0.475 M, 1 eq). The reaction was run in microwave at 140°C for 20 minutes. Hydrolysis with LiOH in 3:1 MeOH/H_2O (0.7 M, 19 mL, 13.3 mmol, 14 eq) afforded brown

solid (99.7 mg, 0.41 mmol, 43% overall yield). ^{1}H-NMR (400 MHz, methanol-d_4): δ (ppm) 8.44 (s, 2H), 7.84 (d, *J* = 6.9 Hz, 2H), 7.56 (m, 3H). ^{13}C-NMR (100 MHz, methanol-d_4): δ (ppm) 164.1, 149.1, 135.3, 131.4, 53.6; LRMS (ESI) calcd for $C_{13}H_9NO_4$: m/z 244.0 (M + H), found: 243.9, retention time = 10.31 min.

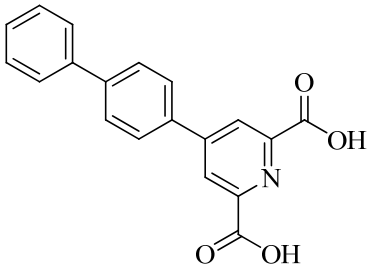

12

4-(Biphenyl-4-yl)pyridine-2,6-dicarboxylic acid (12). Dimethyl 4-bromopyridine-2,6-dicarboxylate **10** (203 mg, 0.74 mmol), biphenyl-4-ylboronic acid (147 mg, 0.74 mmol), Pd(dppf)Cl_2·CH_2Cl_2 (60 mg, 0.074 mmol, 10 mol%), dichloroethane (2 mL), aqueous Cs_2CO_3 (2 mL, 0.37 M, 1 eq). The reaction was run in microwave at 140^{o}C for 30 minutes. Hydrolysis with LiOH in 3:1 MeOH/H_2O (15 mL, 0.7 M, 10.4 mmol, 14 eq) afforded brown solid (83 mg, 0.26 mmol, 35% overall yield). ^{1}H-NMR (400 MHz, DMSO-d_6): δ (ppm) 8.47 (s, 2H), 8.00 (d, *J* = 8.3 Hz, 2H), 7.84 (d, *J* = 8.7 Hz, 2H), 7.73 (d, *J* = 7.4 Hz, 2H), 7.48 (apparent t, *J* = 7.4, 7.8 Hz, 2H), 7.38 (t, *J* = 7.3 Hz, 1H) ; LRMS (ESI) calcd for $C_{19}H_{13}NO_4$: m/z 320.1 (M + H), found: 320.1, retention time = 11.44 min.

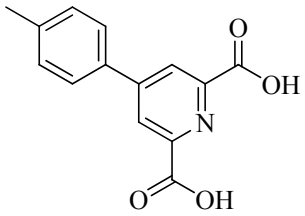

13

4-*p*-Tolylpyridine-2,6-dicarboxylic acid (13). Dimethyl 4-bromopyridine-2,6-dicarboxylate **10** (260 mg, 0.95 mmol), *p*-tolylboronic acid (195 mg, 1.425 mmol, 1.5 eq), $Pd(dppf)Cl_2 \cdot CH_2Cl_2$ (78 mg, 0.095 mmol, 10 mol%), dichloroethane (2.5 mL), aqueous Cs_2CO_3 (2 mL, 0.475 M, 1 eq). The reaction was run in microwave at 140°C for 40 minutes. Hydrolysis with LiOH in 3:1 MeOH/H_2O (19 mL, 0.7 M, 13.3 mmol, 14 eq) afforded brown solid (173 mg, 0.67 mmol, 71% overall yield). ^{1}H-NMR (400 MHz, DMSO-d_6): δ (ppm) 8.39 (s, 2H), 7.78 (d, *J* = 8.2 Hz, 2H), 7.33 (d, *J* = 7.8, 2H), 2.34 (s, 3H). ^{13}C-NMR (100 MHz, DMSO-d_6): δ (ppm) 166.2, 150.3, 150.2, 140.7, 133.5, 130.6, 127.5, 124.4, 21.4; LRMS (ESI) calcd for $C_{14}H_{11}NO_4$: m/z 258.1 (M + H), found: 258.0, retention time = 10.52 min.

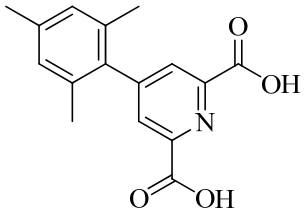

14

4-Mesitylpyridine-2,6-dicarboxylic acid (14). Dimethyl 4-bromopyridine-2,6-dicarboxylate **10** (260 mg, 0.95 mmol), mesitylboronic acid (234 mg, 1.425 mmol, 1.5 eq), $Pd(dppf)Cl_2 \cdot CH_2Cl_2$ (78 mg, 0.095 mmol, 10 mol%), dichloroethane (2.5 mL), aqueous Cs_2CO_3 (2 mL, 0.475 M, 1 eq). The reaction was run in microwave at 140°C for 40 minutes. Hydrolysis with LiOH in 3:1 MeOH/H_2O (19 mL, 0.7 M, 13.3 mmol, 14 eq) afforded white solid (167 mg, 0.58 mmol, 61% overall yield). ^{1}H-NMR (400 MHz, DMSO-d_6): δ (ppm) 7.91 (s, 2H), 6.95 (s, 2H), 2.24 (s, 3H), 1.89 (s, 6H). ^{13}C-NMR (100 MHz, DMSO-d_6): δ (ppm) 166.1, 151.9, 149.4, 138.1, 135.1, 135.0, 128.9, 128.6, 21.2, 20.7; LRMS (ESI) calcd for $C_{16}H_{15}NO_4$: m/z 286.1 (M + H), found: 286.3, retention time = 10.90 min.

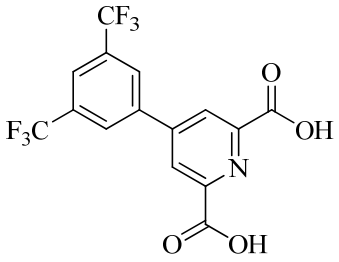

15

4-(3,5-bis(trifluoromethyl)phenyl)pyridine-2,6-dicarboxylic acid (15). Dimethyl 4-bromopyridine-2,6-dicarboxylate **10** (200 mg, 0.74 mmol), 3,5-bis(trifluoromethyl)phenyl boronic acid (191 mg, 0.74 mmol, 1 eq), $Pd(dppf)Cl_2 \cdot CH_2Cl_2$ (60 mg, 0.074 mmol, 10 mol%), dichloroethane (2 mL), aqueous Cs_2CO_3 (2 mL, 0.37 M, 1 eq). The reaction was run in microwave at 120°C for 10 minutes. Hydrolysis with LiOH in 3:1 MeOH/H_2O (15 mL, 0.7 M, 10.4 mmol, 14 eq) afforded white solid (3 mg, 7.9 μmol, 1% overall yield). ^{1}H-NMR (400 MHz, methanol-d_4): δ (ppm) 8.65 (s, 2H), 8.43 (s, 2H), 8.15 (s, 1H); LRMS (ESI) calcd for $C_{15}H_7F_6NO_4$: m/z 380.0 (M + H), found: 397.7 (100), 380.3 (93), retention time = 11.36 min.

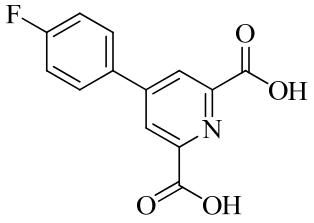

16

4-(4-Fluorophenyl)pyridine-2,6-dicarboxylic acid (16). Dimethyl 4-bromopyridine-2,6-dicarboxylate **10** (260 mg, 0.95 mmol), 4-fluorophenylboronic acid (200 mg, 1.425 mmol, 1.5 eq), $Pd(dppf)Cl_2 \cdot CH_2Cl_2$ (78 mg, 0.095 mmol, 10 mol%), dichloroethane (2.5 mL), aqueous Cs_2CO_3 (2 mL, 0.475 M, 1 eq). The reaction was run in microwave at 140°C for 40 minutes. Hydrolysis with LiOH in 3:1 MeOH/H_2O (19 mL, 0.7 M, 13.3 mmol, 14 eq)

afforded off-white solid (151 mg, 0.52 mmol, 27% overall yield). ^{1}H-NMR (400 MHz, methanol-d_4): δ (ppm) 8.57 (s, 2H), 7.90 (dd, *J* = 8.7 Hz, 2H), 7.30 (t, *J* = 8.7 Hz, 2H); LRMS (ESI) calcd for $C_{18}H_8FNO_4$: m/z 262.1 (M + H), found: 261.8, retention time = 10.22 min.

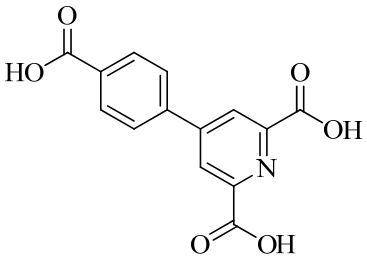

17

4-(4-Carboxyphenyl)pyridine-2,6-dicarboxylic acid (17). Dimethyl 4-bromopyridine-2,6-dicarboxylate **10** (260 mg, 0.95 mmol), 4-boronobenzoic acid (315 mg, 1.9 mmol, 2 eq), Pd(dppf)Cl_2·CH_2Cl_2 (78 mg, 0.095 mmol, 10 mol%), dichloroethane (2.5 mL), aqueous Cs_2CO_3 (2 mL, 0.475 M, 1 eq). The reaction was run in microwave at 140^{o}C for 40 minutes. Hydrolysis with LiOH in 3:1 MeOH/H_2O (19 mL, 0.7 M, 13.3 mmol, 14 eq) afforded white solid (76 mg, 0.26 mmol, 28% overall yield). ^{1}H-NMR (400 MHz, methanol-d_4): δ (ppm) 8.48 (s, 2H), 8.04 (apparent q, *J* = 8.7 Hz, 4H); LRMS (ESI) calcd for $C_{14}H_9NO_6$: m/z 288.1 (M + H), found: 288.0, retention time = 9.55 min.

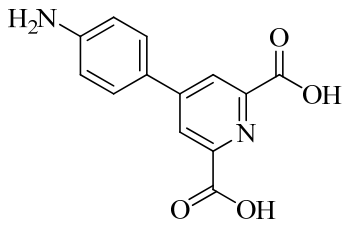

18

4-(4-Aminophenyl)pyridine-2,6-dicarboxylic acid (18). Dimethyl 4-bromopyridine-2,6-dicarboxylate **10** (260 mg, 0.95 mmol), 4-(4,4,5,5-tetramethyl-1,3,2-dioxaborolan-2-yl)aniline (312 mg, 1.425 mmol, 1.5 eq), $Pd(dppf)Cl_2 \cdot CH_2Cl_2$ (78 mg, 0.095 mmol, 10 mol%), dichloroethane (2.5 mL), aqueous Cs_2CO_3 (2 mL, 0.475 M, 1 eq). The reaction was run in microwave at 140°C for 40 minutes. Hydrolysis with LiOH in 3:1 MeOH/H_2O (19 mL, 0.7 M, 13.3 mmol, 14 eq) afforded yellow solid (pending). ^{1}H-NMR (400 MHz, methanol-d_4): δ (ppm) 8.31 (s, 2H), 7.61 (d, J = 8.7 Hz, 2H), 6.79 (d, J = 8.7 Hz, 2H); LRMS (ESI) calcd for $C_{13}H_{10}N_2O_4$: m/z 259.1 (M + H), found: 258.9, retention time = 9.09 min.

5. References

1. J. A. Littlechild, *J. Phys. D: Appl. Phys.*, **1991**, *24*, 111–118.
2. A. McPherson, *Methods*, **2004**, *34*, 254–265.
3. M. A. Dessau, Y. Modis, *J. Vis. Exp.*, **2011**, *47*, e2285, doi: 10.3791/2285.
4. N. E. Chayen, E. Saridakis, *Acta Cryst.*, **2002**, *D58*, 921–927.
5. A. McPherson, C. Nguyen, R. Cudney, S. B. Larson, *Cryst. Growth Des.*, **2011**, *11*, 1469–1474, and references within.
6. H. P. Morgan, I. W. McNae, K-Y. Hsin, P. A. M. Michels, L. A. Fothergill-Gilmore, M. D. Walkinshaw, *Acta Cryst.*, **2010**, *F66*, 215–218.
7. S. Patel, B. Cudney, A. McPherson, *Biochem. Biophys. Res. Commun.*, **1995**, *207*, 819–828.
8. T-C. Hu, J. Korczyńska, D. K. Smith, A. M. Brzozowski, *Acta Cryst.*, **2008**, *D64*, 957–963.
9. E. N. Salgado, J. Faraone-Mennella, F. A. Tezcan, *J. Am. Chem. Soc.*, **2007**, *129*, 13374–13375.
10. E. N. Salgado, R. J. Radford, F. A. Tezcan, *Acc. Chem. Res.*, **2010**, *43*, 661–672.
11. S. B. Larson, J. S. Day, R. Cudney, A. McPherson, *Acta Cryst.*, **2007**, *D63*, 310–318.
12. G. Pompidor, A. D'Aléo, J. Vicat, L. Toupet, N. Giraud, R. Kahn, O. Maury, *Angew. Chem.*, **2008**, *120*, 3436–3439; *Angew. Chem. Int. Ed.*, **2008**, *47*, 3388–3391.
13. G. Pompidor, O. Maury, J. Vicat, R. Kahn, *Acta Cryst.*, **2010**, *D66*, 762–769.
14. R. Talon, L. Nauton, J-L. Canet, R. Kahn, E. Girard, A. Gautier, *Chem. Commun.*, **2012**, *48*, 11886-11888.

15. a) E. Girard, L. Chantalat, J. Vicat, R. Kahn, *Acta Cryst.*, **2002**, *D58*, 1–9; b) E. Girard, M. Steller, P. L. Anelli, J. Vicat, R. Kahn, *Acta Cryst.*, **2003**, *D59*, 118–126; c) E. Girard, P. L. Anelli, J. Vicat, R. Kahn, *Acta Cryst.*, **2003**, *D59*, 1877–1880; d) E. Girard, M. Stelter, J. Vicat, R. Kahn, *Acta Cryst.*, **2003**, *D59*, 1914–1922.

16. A. Suzuki, *Angew. Chem.*, **2011**, *123*, 6854–6869; *Angew. Chem. Int. Ed.*, **2011**, *50*, 6722–6737.

17. P. M. J. Lory, A. Agarkov, S. R. Gilbertson, *Synlett*, **2006**, *(18)*, 3045–3048.

18. S. Lundgren, S. Lutsenko, C. Jonsson, C. Moberg, *Org. Lett.*, **2003**, *5*, 3663–3665.

19. T. Korenaga, T. Kosaki, R. Fukumura, T. Ema, T. Sakai, *Org. Lett.*, **2005**, *7*, 4915–4917.

20. Alternatively, after cooling to room temperature, the solvents were removed. The crude material was flashed through silica gel in hexane/EtOAc.

6. NMR spectra

Dimethyl 4-bromopyridine-2,6-dicarboxylate (**10**)

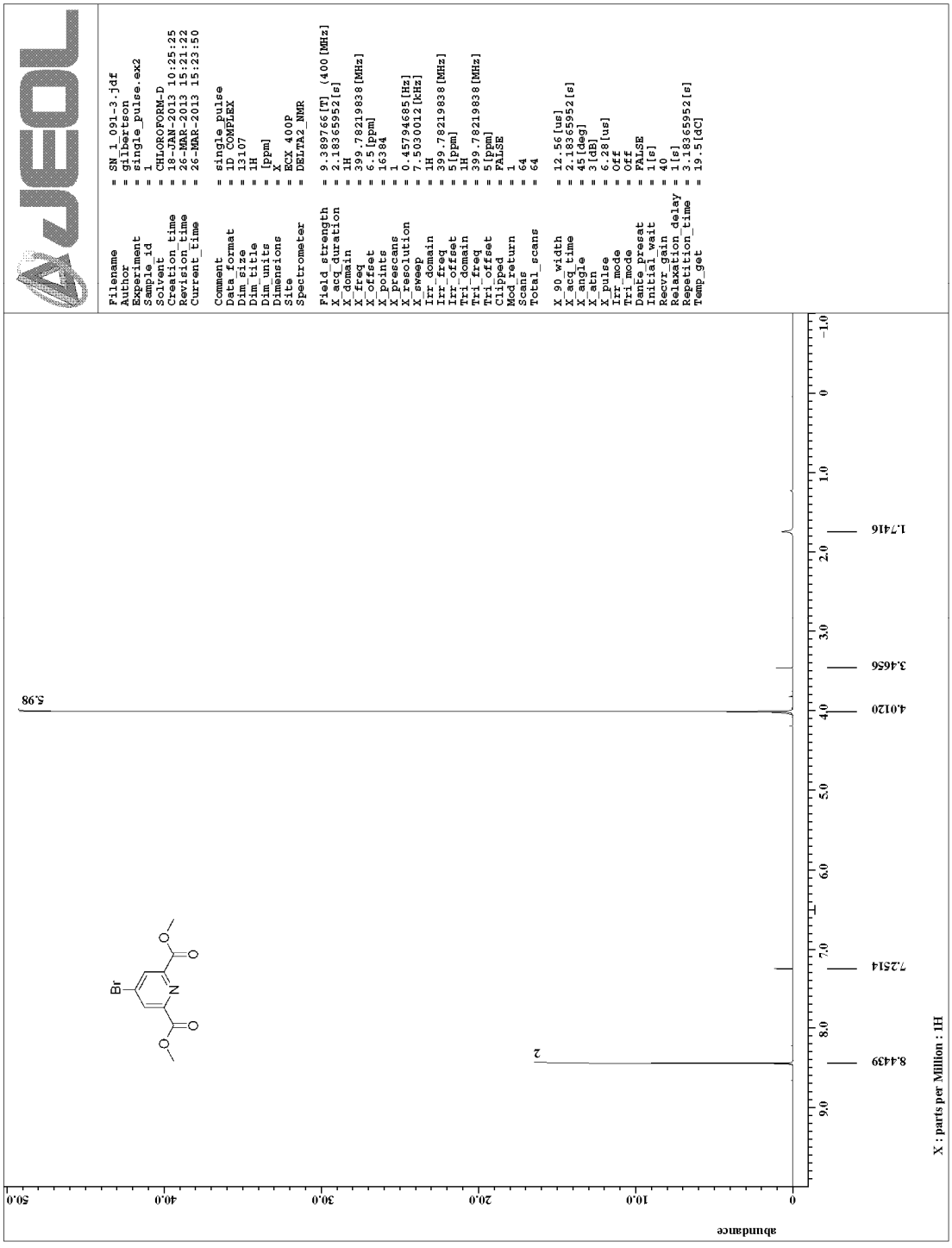

Dimethyl 4-bromopyridine-2,6-dicarboxylate (**10**)

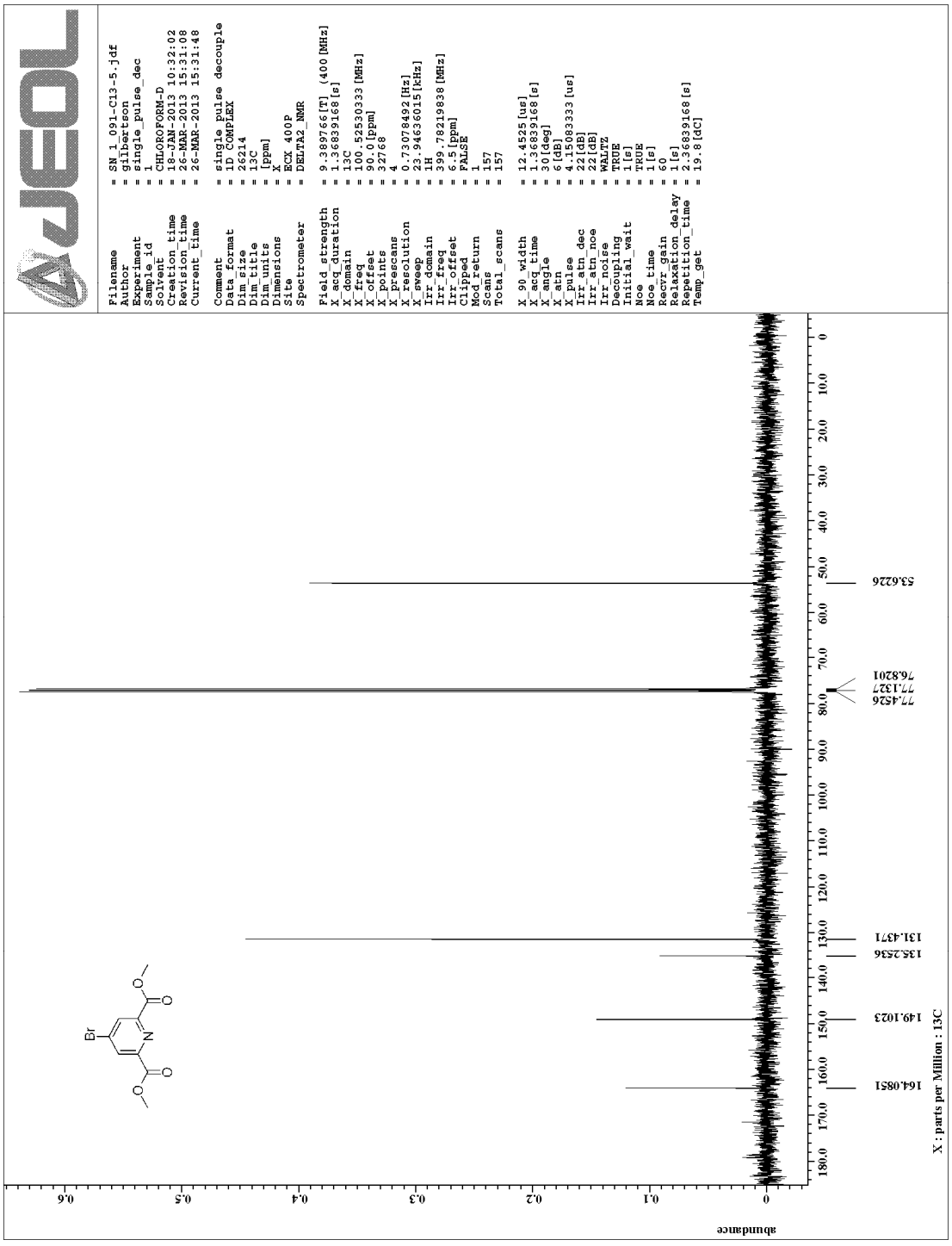

4-Phenylpyridine-2,6-dicarboxylic acid (**11**)

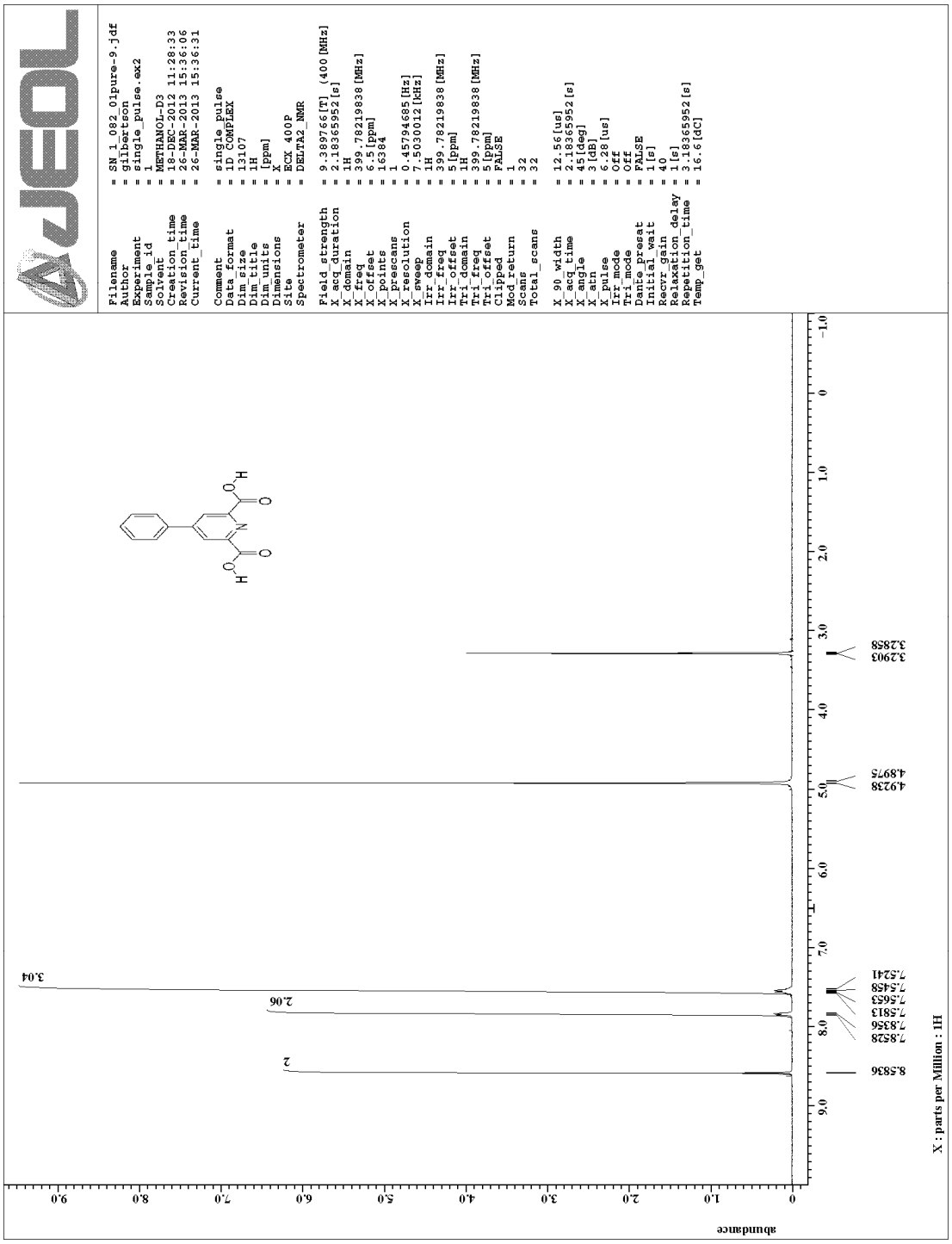

4-(Biphenyl-4-yl)-pyridine-2,6-dicarboxylic acid (**12**)

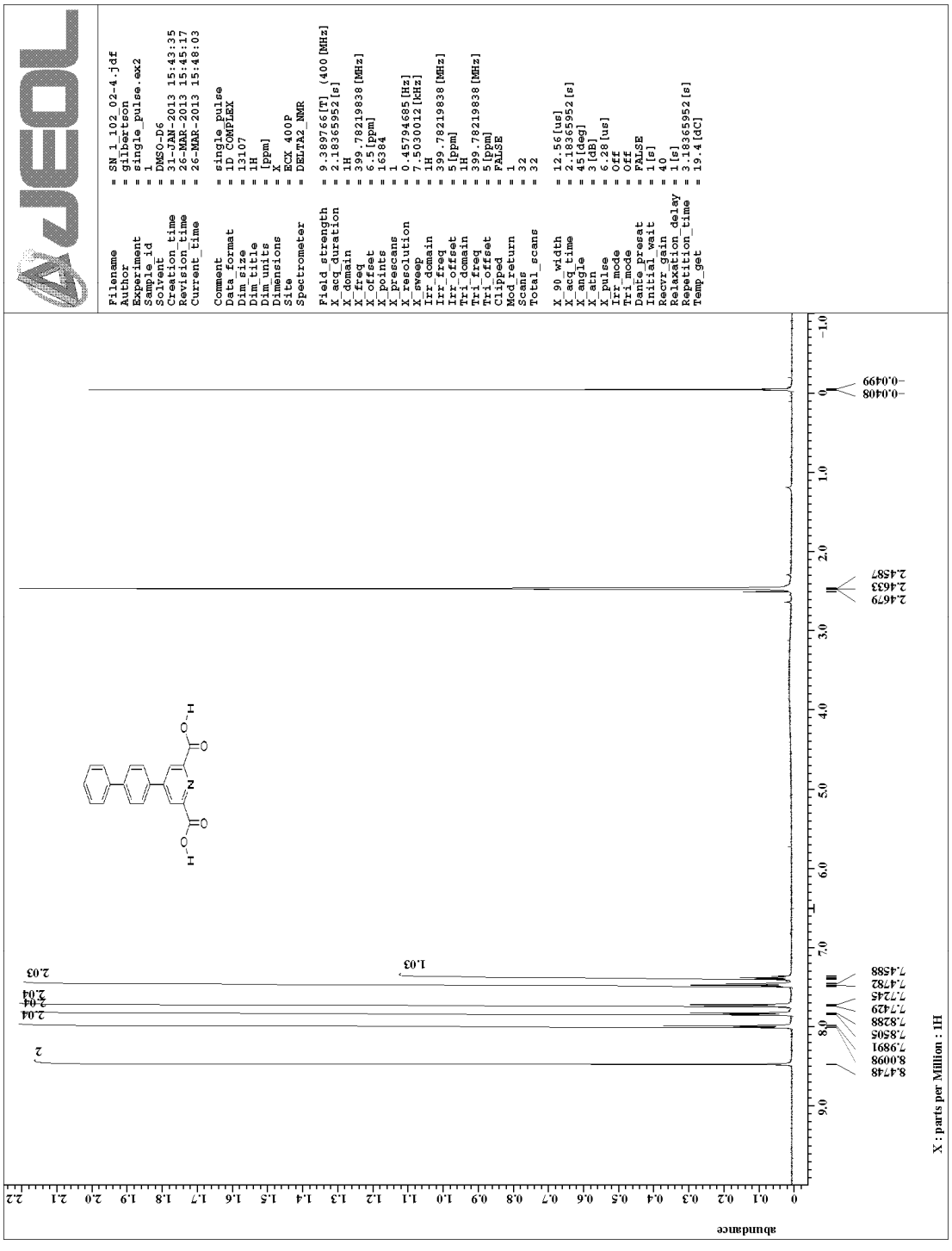

4-*p*-Tolylpyridine-2,6-dicarboxylic acid (**13**)

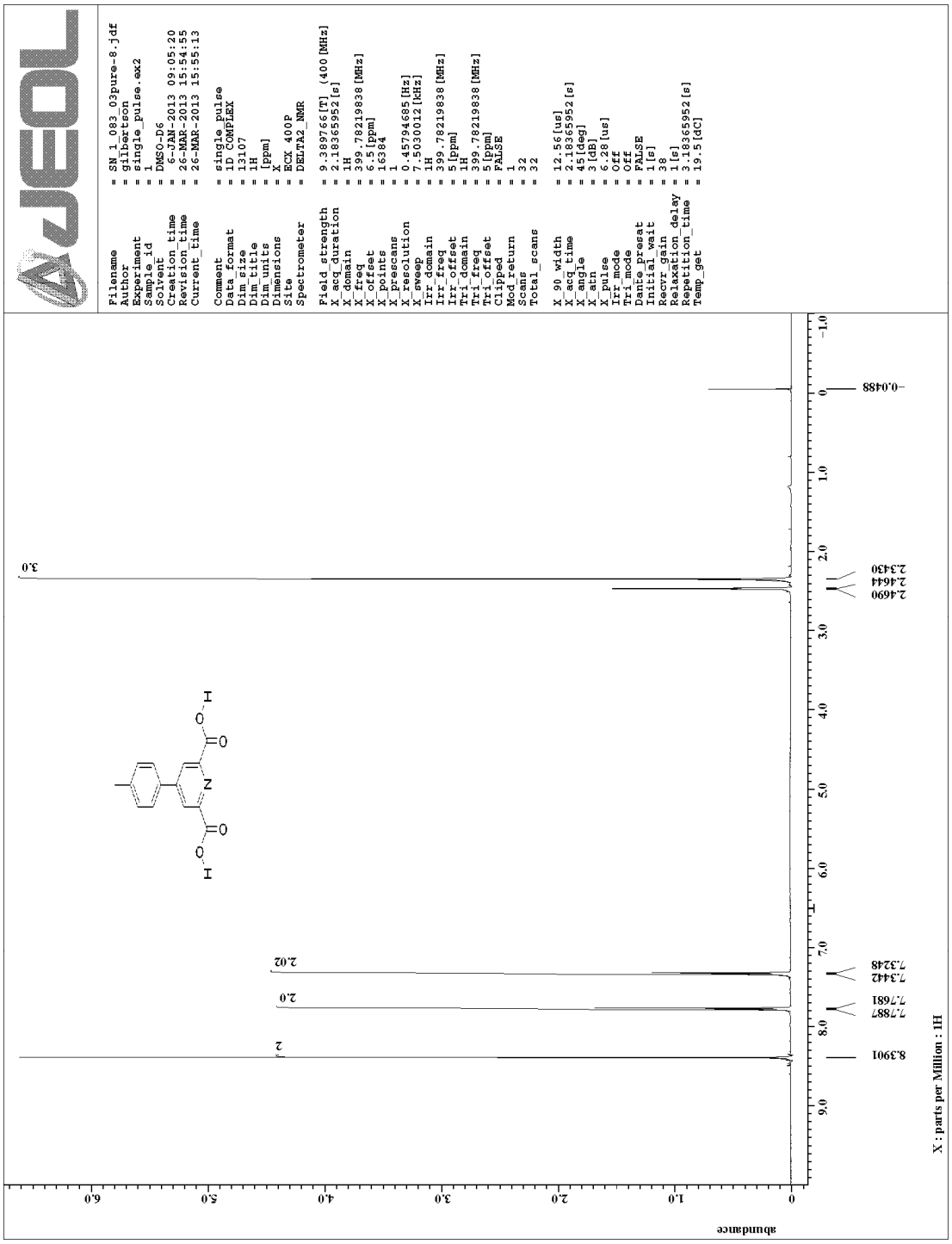

4-*p*-Tolylpyridine-2,6-dicarboxylic acid (**13**)

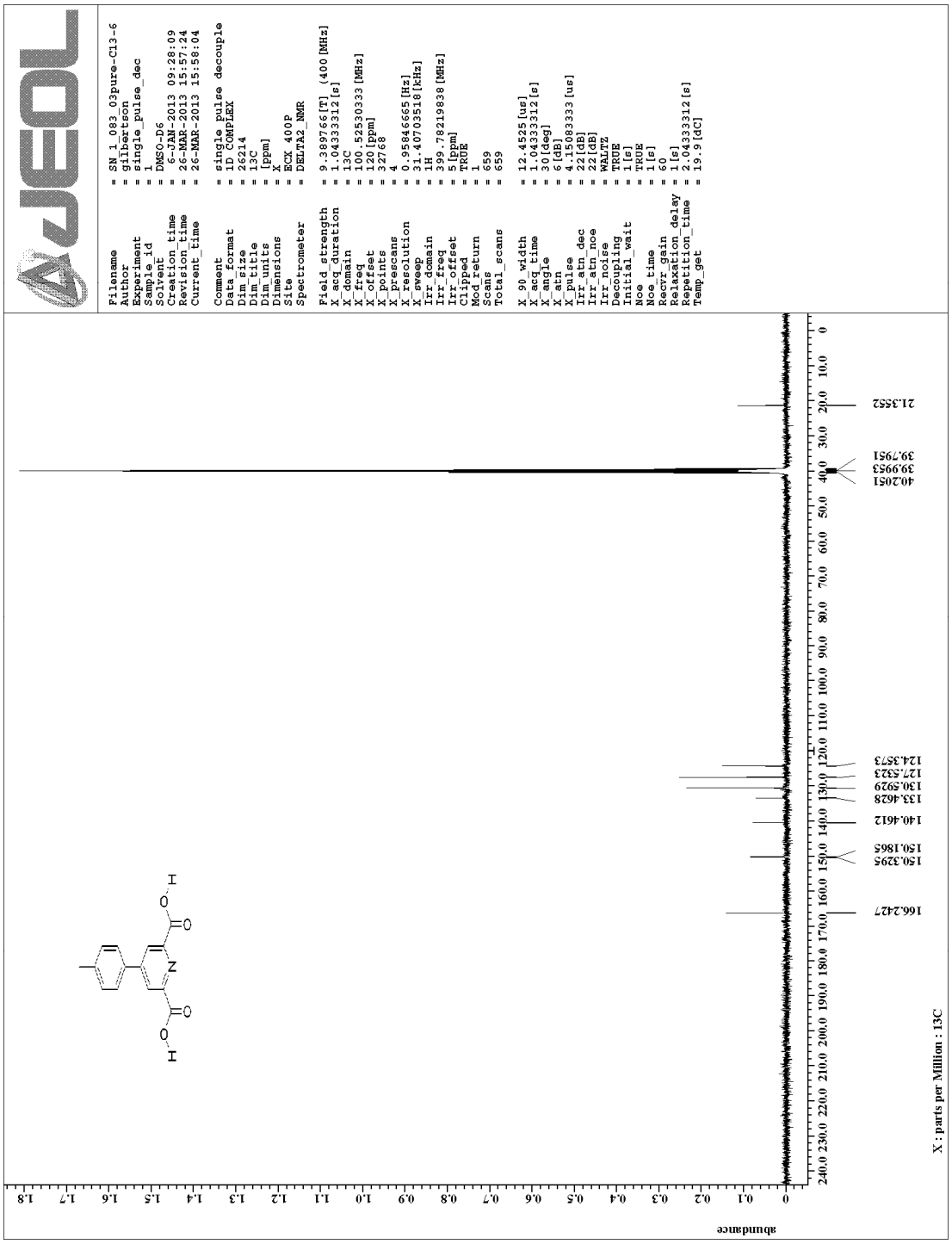

4-Mesitylpyridine-2,6-dicarboxylic acid (**14**)

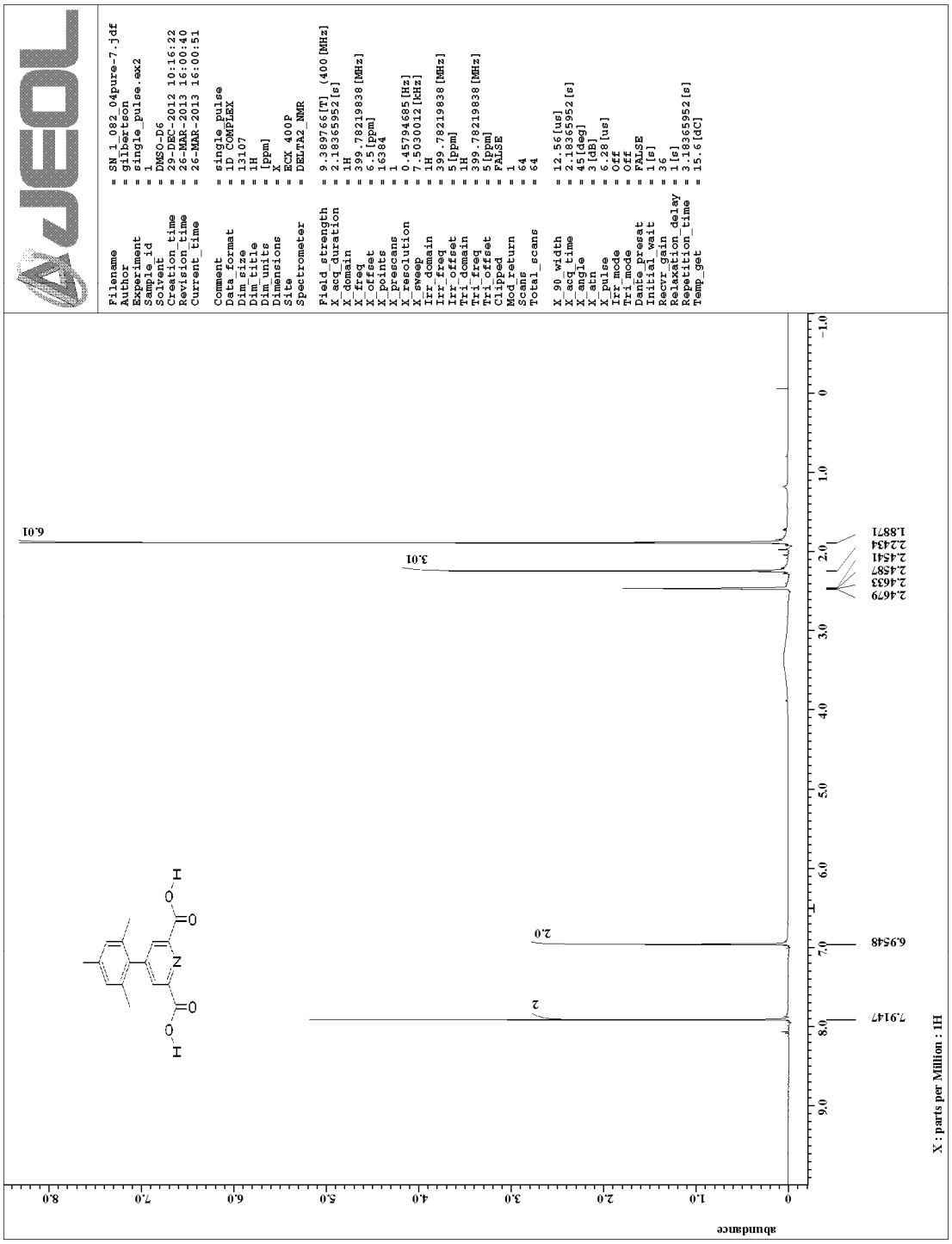

4-Mesitylpyridine-2,6-dicarboxylic acid (**14**)

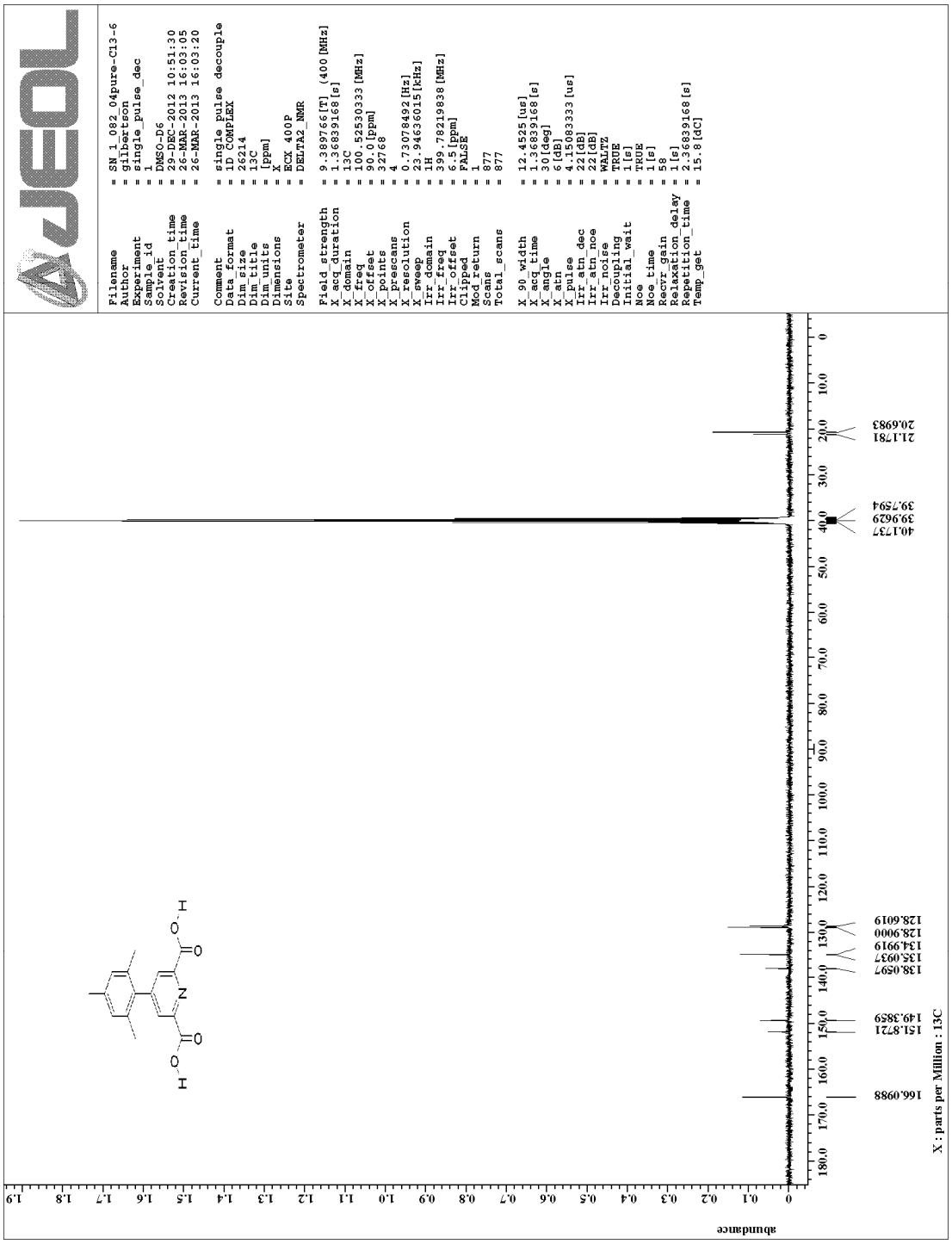

4-(3,5-bis(Trifluoromethyl)phenyl)pyridine-2,6-dicarboxylic acid (**15**)

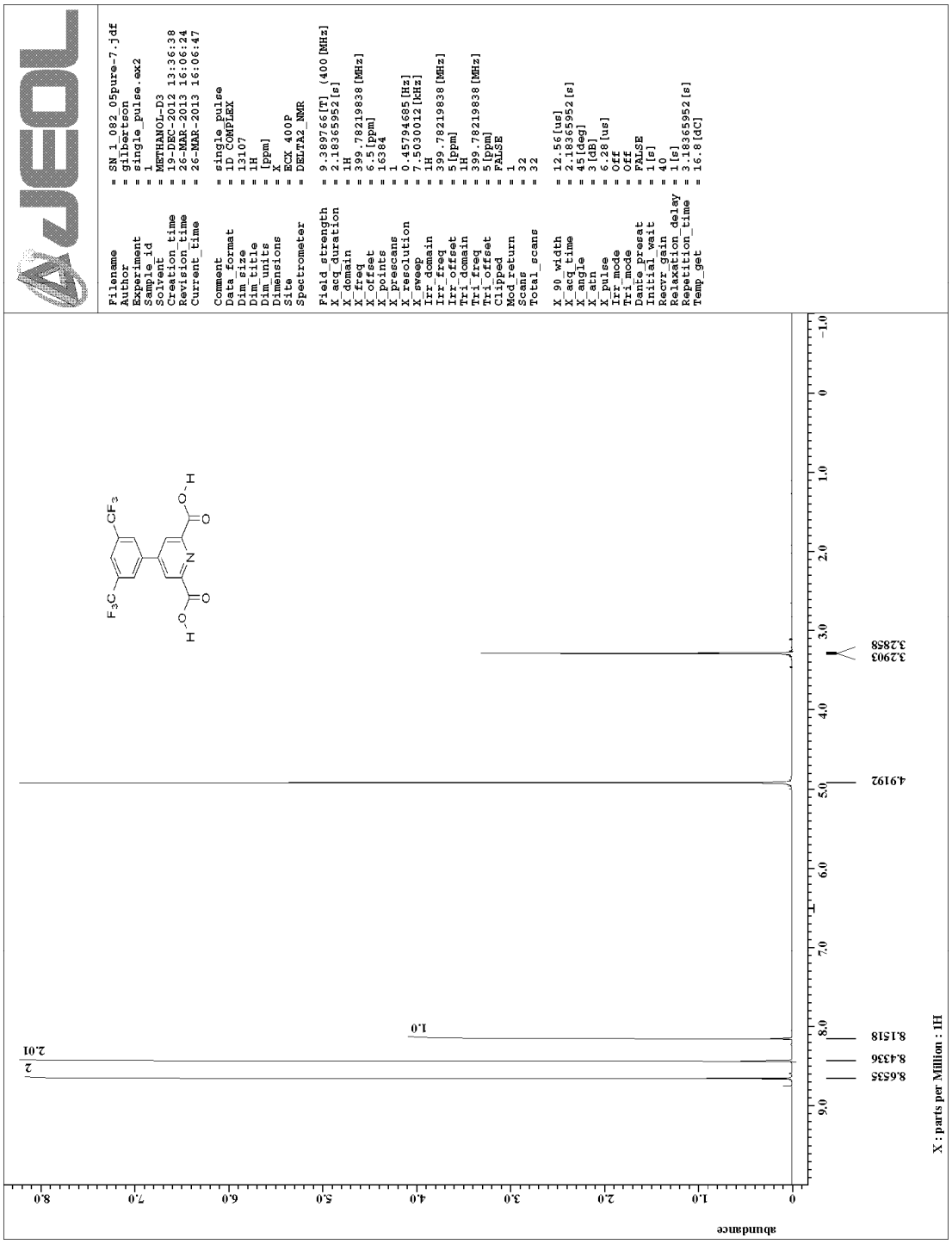

4-(4-Fluorophenyl)pyridine-2,6-dicarboxylic acid (**16**)

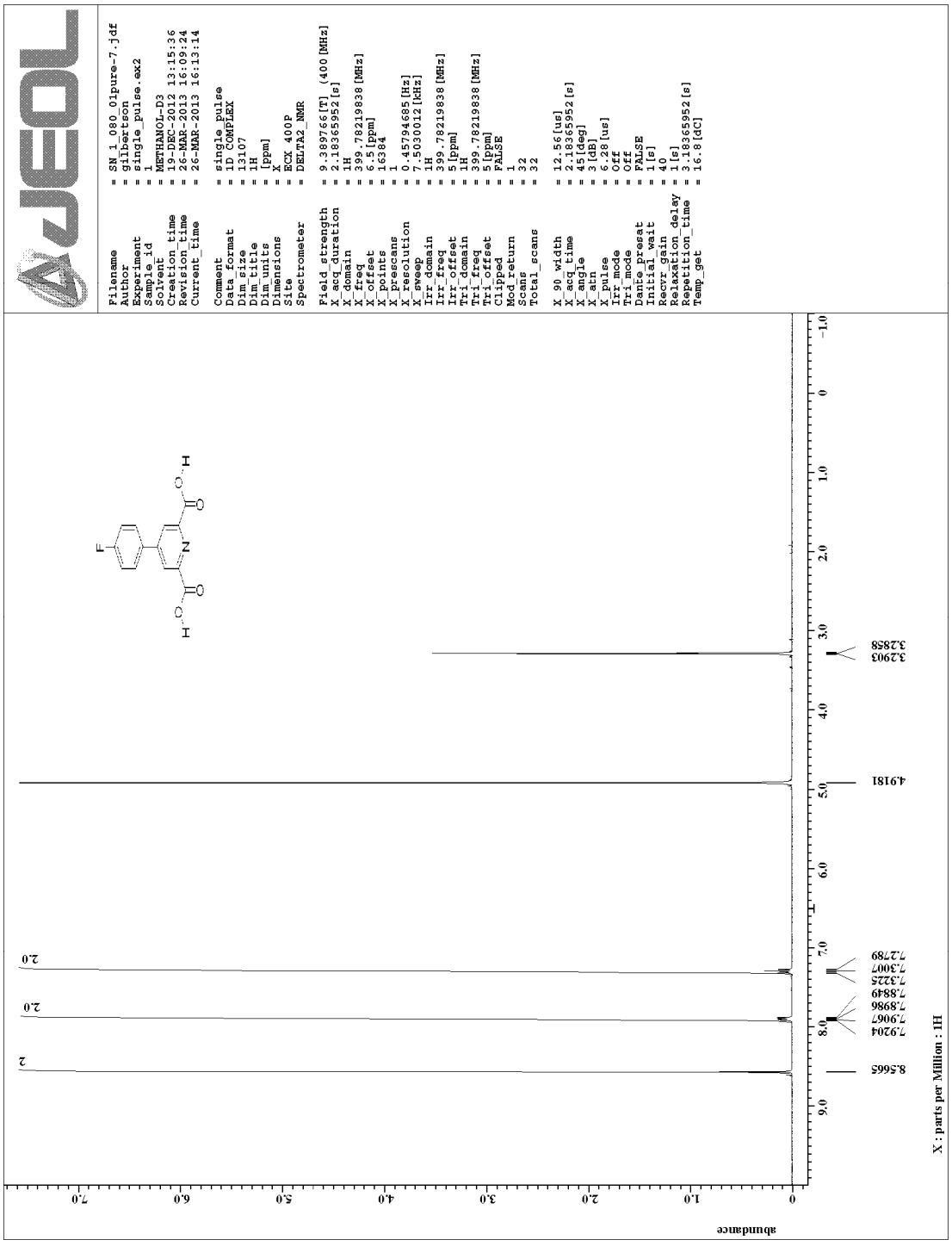

4-(4-Carboxyphenyl)pyridine-2,6-dicarboxylic acid (**17**)

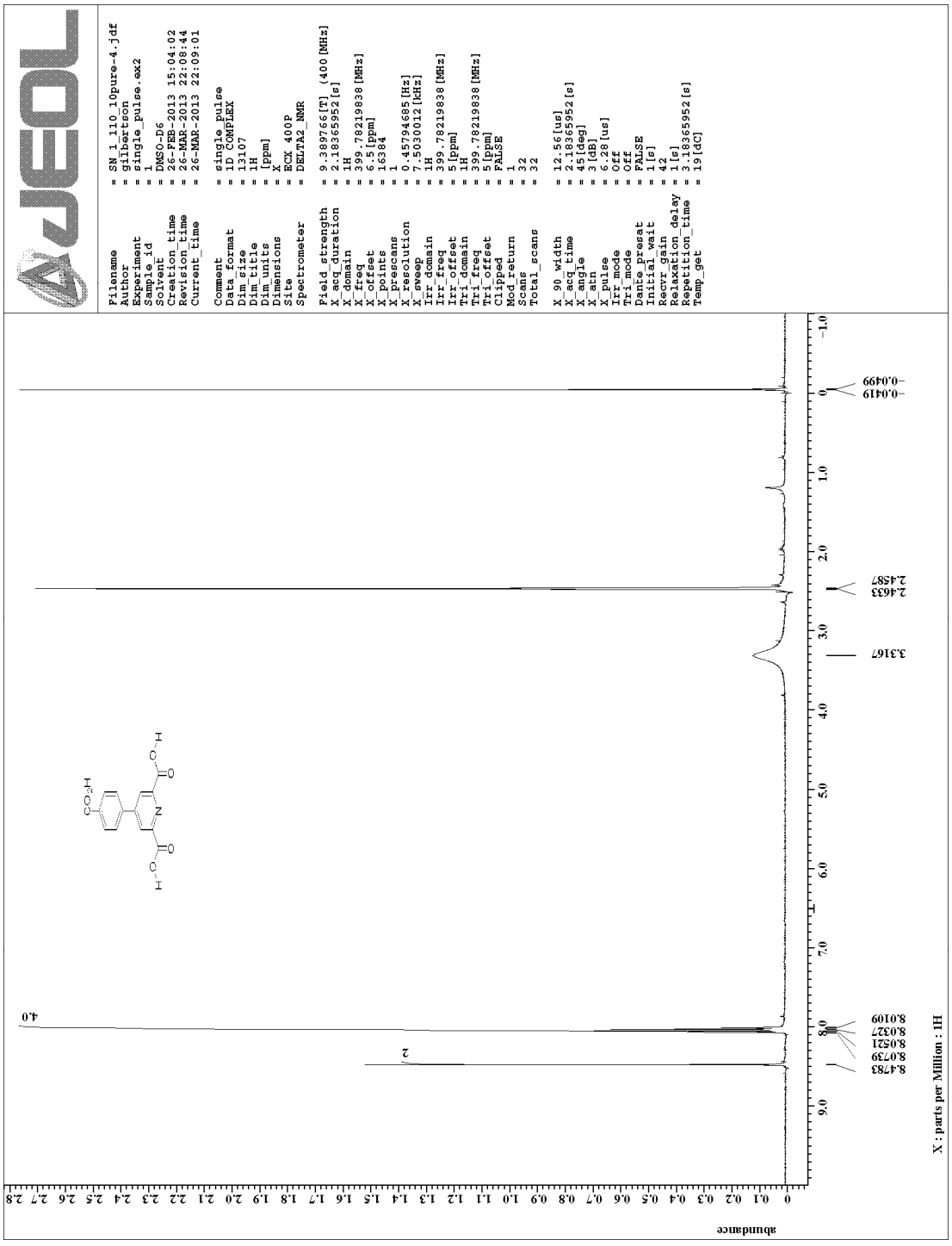

4-(4-Aminophenyl)pyridine-2,6-dicarboxylic acid (**18**)